

Reconstruction of the primordial power spectra with Planck and BICEP2 data

Bin Hu,^{1,*} Jian-Wei Hu,^{2,†} Zong-Kuan Guo,^{2,‡} and Rong-Gen Cai^{2,3,§}

¹*Institute Lorentz of Theoretical Physics, University of Leiden, 2333CA Leiden, The Netherlands*

²*State Key Laboratory of Theoretical Physics, Institute of Theoretical Physics, Chinese Academy of Sciences, P.O. Box 2735, Beijing 100190, China*

³*King Abdulaziz University, Jeddah 21589, Saudi Arabia*

(Received 23 April 2014; published 30 July 2014)

By using the cubic spline interpolation method, we reconstruct the shape of the primordial scalar and tensor power spectra from the recently released Planck temperature and BICEP2 polarization cosmic microwave background data. We find that the vanishing scalar index running ($dn_s/d\ln k$) model is strongly disfavored at more than 3σ confidence level on the $k = 0.0002 \text{ Mpc}^{-1}$ scale. Furthermore, the power-law parametrization gives a blue-tilt tensor spectrum, no matter using only the first five bandpowers $n_t = 1.20^{+0.56}_{-0.64}$ (95% C.L.) or the full nine bandpowers $n_t = 1.24^{+0.51}_{-0.58}$ (95% C.L.) of BICEP2 data sets. Unlike the large tensor-to-scalar ratio value ($r \sim 0.20$) under the scale-invariant tensor spectrum assumption, our interpolation approach gives $r_{0.002} < 0.060$ (95% C.L.) by using the first five bandpowers of BICEP2 data. After comparing the results with/without BICEP2 data, we find that Planck temperature with small tensor amplitude signals and BICEP2 polarization data with large tensor amplitude signals dominate the tensor spectrum reconstruction on the large and small scales, respectively. Hence, the resulting blue tensor tilt actually reflects the tension between Planck and BICEP2 data.

DOI: [10.1103/PhysRevD.90.023544](https://doi.org/10.1103/PhysRevD.90.023544)

PACS numbers: 98.80.Cq, 98.80.-k

I. INTRODUCTION

Recently, the BICEP2 experiment [1] reported an excess of cosmic microwave background (CMB) B-mode polarization power spectrum over the base lensed- Λ CDM expectation in the range $30 < \ell < 150$, inconsistent with the null hypothesis at a significance of $> 5\sigma$. Since the single field slow-roll inflationary model predicts a peak around multipole $\ell \sim 80$ in the B-mode autocorrelation (BB) spectrum seeded by the primordial gravitational wave/tensor perturbation mode, the BICEP2 results are believed to be the first indirect detection of the primordial gravitational wave. Under the assumption of power-law scalar and scale-invariant tensor spectra, the observed B-mode power spectrum is well described by a lensed- Λ CDM + tensor theoretical model with tensor-to-scalar ratio $r = 0.20^{+0.07}_{-0.05}$ with $r = 0$ disfavored at the 7.0σ confidence level.

However, the scientific results of BICEP2 data are in tension with those from other CMB experiments, such as Planck [2]. The first discrepancy is in the amplitude of the scale-invariant tensor spectrum, which is described by the tensor-to-scalar ratio $r \equiv A_t/A_s$. Unlike the scalar perturbations, due to the absence of acoustic oscillation mechanism the tensor contributions to the temperature CMB spectrum are rapidly washed out inside the horizon at

electron-proton recombination epoch ($\ell \geq 200$) [3]. Hence, the temperature anisotropies on the large scales are the mixture of scalar and tensor contributions. Furthermore, if one assumes the simple power-law form of the primordial scalar power spectrum, i.e. no scalar index running $dn_s/d\ln k = 0$, the precisely measured higher multipoles by Planck put stringent constraints on the scalar amplitude A_s and index n_s . Therefore, in order to explain the observed power deficit in the low- ℓ regime by Planck, one has to suppress the tensor spectrum amplitude. Consequently, from only the temperature anisotropy measured by Planck, one has $r < 0.11$ at 95%, which is in a “very significant” tension (around 0.1% unlikely) with BICEP2 results [4]. As stressed by the BICEP2 team, however, this tension could be reconciled by adding the running of the scalar index which is the degree of freedom to suppress the scalar temperature anisotropy in the low- ℓ regime. Then, combining Planck with WMAP low- ℓ polarization [5] and ACT [6]/SPT [7–9] high- ℓ data, one could get $r < 0.26$ at 95%. Besides that, several other possible solutions to this tension have been proposed, such as step feature spectra [10–12], fast-slow roll model [13], anticorrelation scalar isocurvature initial condition [14,15], sterile neutrino species [16–18], sudden change in speed of inflaton or Lorentz violation [19]. See also [20–25] for other possibilities.

The second tension is between the observed blue-tilt tensor spectrum ($n_t > 0$) [26–30] by BICEP2 and the red-tilt one ($n_t = -r/8$) predicted by the standard inflationary paradigm. Generally, the blue tensor spectrum asks for violation of the null energy condition (NEC), which

* hu@lorentz.leidenuniv.nl

† jwhu@itp.ac.cn

‡ guozk@itp.ac.cn

§ cairg@itp.ac.cn

is equivalent to $\rho + P < 0$ (or $\dot{H} > 0$) in the flat universe. There exist several NEC violation inflationary models in the literature, such as super inflation [31], phantom inflation [32], G-inflation [33], etc. Some alternative paradigm of inflation, such as “string gas cosmology” [34], bouncing universe [35–41] or other possibilities [42,43] (see the references therein) might be helpful to solve this tension.

In this paper, we start from a purely phenomenological point of view to reconstruct the shape of primordial scalar and tensor spectra from Planck temperature and BICEP2 polarization data.

II. PARAMETRIZATION OF PRIMORDIAL SPECTRA AND DATA SETS

In order to reconstruct a smooth spectrum with the continuous first and second derivatives, in this paper we adopt the cubic spline interpolation method, which has been used to analyze WMAP or Planck temperature and polarization data [44–51]. Besides the cubic spline interpolation reconstruction, there also exist other model independent algorithms, such as Bayesian evidence selected linear interpolation [52,53]. Due to the fact that the amplitude of CMB anisotropy is so tiny, $\delta T/\bar{T} \sim \mathcal{O}(10^{-5})$, and CMB observational windows cover several orders of magnitude in spatial scale, it is reasonable to parametrize the logarithms of primordial spectra, which seed the CMB anisotropy, in the logarithms of fluctuation wave number, $\ln k$. The method of cubic spline interpolation can be summarized as follows.

First, we uniformly sample N_{bin} points in the logarithmic scale of wave number. Second, inside of the sampled bins $\ln k_i < \ln k < \ln k_{i+1}$, we use the cubic spline interpolation to determine logarithmic values of the primordial power spectrum. Third, the boundary conditions are adopted, where the second derivative is set to zero. For $k < k_1$ or $k > k_{N_{\text{bin}}}$ we fix the slope of the primordial power spectrum at the boundaries and linearly extrapolate to the outside regimes. Mathematically, the corresponding formula could be written as

$$\ln \mathcal{P}(k) = \begin{cases} \left. \frac{d \ln \mathcal{P}(k)}{d \ln k} \right|_{k_1} \ln \frac{k}{k_1} + \ln \mathcal{P}(k_1), & k < k_1; \\ \ln \mathcal{P}(k_i), & k \in \{k_i\}; \\ \text{cubic spline,} & k_i < k < k_{i+1}; \\ \left. \frac{d \ln \mathcal{P}(k)}{d \ln k} \right|_{k_{N_{\text{bin}}}} \ln \frac{k}{k_{N_{\text{bin}}}} + \ln \mathcal{P}(k_{N_{\text{bin}}}), & k > k_{N_{\text{bin}}}. \end{cases} \quad (1)$$

This reconstruction method has three advantages: first of all, it is easy to detect deviations from a scale-invariant spectrum or a power-law spectrum because both the scale-invariant and power-law spectra are just straight lines in the $\ln \mathcal{P} - \ln k$ plane. Second, negative values of the spectrum can be avoided by using $\ln \mathcal{P}(k)$ instead of $\mathcal{P}(k)$ for splines

with steep slopes. Finally, the shape of the power spectrum reduces to the scale-invariant or power-law spectrum as a special case when $N_{\text{bin}} = 1, 2$, respectively.

Since the purpose of this work is to reconstruct the scalar and tensor spectra, we need to adopt different sampling logarithms based on the different observational windows. For the primordial scalar curvature spectrum, its constraints are mainly driven by the CMB temperature modes. With Planck sensitivities, we uniformly sample three bins ranged in $\ln k \in (-8.517, -1.609)$, which corresponds to $k \in (0.0002, 0.2) \text{ Mpc}^{-1}$. For the tensor spectrum, we adopt two uniformly logarithmic sampling strategies, one is corresponding to the scales $k \in (0.002, 0.03) \text{ Mpc}^{-1}$, the other is $k \in (0.002, 0.02) \text{ Mpc}^{-1}$. This is because the BICEP2 B-mode polarization data, which is a very sensitive probe for the primordial tensor spectrum, have an excess of B-mode power in the range of polar angle multipoles ($20 \leq \ell \leq 340$). Moreover, compared with the first five bandpowers, which is in the range of ($20 \leq \ell \leq 200$), the power in the second four bandpowers has extraordinary excess over the base lensed- Λ CDM expectation. This extraordinary excess might arise from the exotic physical origin beyond standard inflationary paradigm or from some unresolved foreground contaminations. Given this consideration, in this paper we take two different choices of BICEP2 data, the first is using the full nine bandpowers, and the second is to use the selected first five bandpowers. Hence, we have to adjust our sampling logarithms as mentioned above.

In the left part of this section, we would like to briefly review the data sets we used. First of all, we utilize the Planck temperature-temperature power spectra, namely, for low- ℓ modes ($2 \leq \ell < 50$) via all the nine frequency channels ranged from 30–353 GHz, for high- ℓ modes ($50 \leq \ell \leq 2500$) through 100, 143, and 217 GHz frequency channels¹ [54,55]. Second, in order to break the well-known parameter degeneracy between the reionization optical depth and the amplitude of CMB temperature anisotropy, we also include WMAP9 low- ℓ temperature/polarization spectra ($2 \leq \ell \leq 32$) [5]. In addition, we use BICEP2 polarization (EE, EB, BB) spectra from nine (or five) bandpowers of multipoles in ($20 \leq \ell \leq 340$ or 200) of 150 GHz channels [1].² For the data analysis numerical package, we compute the CMB angular power spectra by using the public Einstein-Boltzmann solver CAMB [56] and explore the cosmological parameter space with a Markov Chain Monte Carlo sampler, namely COSMOMC [57].

III. RESULTS AND DISCUSSIONS

In this section we will start with the scalar spectrum reconstruction, and then turn to the tensor spectrum case.

¹<http://pla.esac.esa.int/pla/aio/planckProducts.html>

²<http://www.cfa.harvard.edu/CMB/bicep2/papers.html>

TABLE I. List of the primordial spectrum parameters used in the Monte Carlo sampling.

| Parameter | Range (min, max) |
|---------------------|-------------------------|
| $\ln(10^{10}A_s^2)$ | (2.7,4.0) |
| n_s | (0.9,1.1) |
| $dn_s/d \ln k$ | (-1.0, 1.0) |
| $r_{0.05}$ | (0.0,2.0) |
| n_r | (-1.0, 5.0) |
| $\ln(10^{10}A_1)$ | (1.0,5.0) |
| $\ln(10^{10}A_2)$ | (1.0,5.0) |
| $\ln(10^{10}A_3)$ | (1.0,5.0) |
| $\ln(10^{10}B_1)^a$ | (-3.0, 3.0)/(-3.0, 3.0) |
| $\ln(10^{10}B_2)^a$ | (-2.0, 5.0)/(-3.0, 3.0) |
| $\ln(10^{10}B_3)^a$ | (-1.0, 5.0)/(-3.0, 3.0) |

^aThe left parameter ranges are for the chains from Planck + WP + BICEP2 data compilation, while the right ones are for those without BICEP2 data.

The prior ranges of the primordial spectrum parameters we studied are listed in Table I. Here we emphasize that the differences in the prior of tensor spectra amplitude at our cubic spline sampling knots when BICEP2 data are included, lie in the tension between Planck and BICEP2 data (we will show later). When our Markov-Chain Monte Carlo sampler investigates the wide parameter space spanned by $(\ln B_1, \ln B_2, \ln B_3)$, at some points the resulting spectra are inconsistent with Planck TE cross-correlation data; in order to avoid this problem we have to adjust the prior ranges. But still the widths of the priors are large enough and also the tensor amplitudes $(\ln B_1, \ln B_2, \ln B_3)$ get well constrained in these prior ranges as shown in Fig. 9. So, we conclude that our prior choices will not affect the results significantly.

A. Scalar spectrum reconstruction

Since the main capability of scalar spectrum reconstruction is driven by the CMB temperature data, we first study the case without BICEP2 polarization, i.e. the case with only Planck temperature and WMAP9 low- ℓ polarization (WP) data sets. As mentioned in the previous section, here we uniformly sample three points in the logarithmic scale of wave number, which are located at $k_1 = 0.0002$, $k_2 = 0.0063$ and $k_3 = 0.2 \text{ Mpc}^{-1}$ with the logarithmic amplitudes $\ln A_1$, $\ln A_2$ and $\ln A_3$, respectively. Then, we sample the parameter space spanned by vanilla ΛCDM parameters without the scalar amplitude $\ln A_s$ and its index tilt n_s and replacing them with $\ln A_1$, $\ln A_2$ and $\ln A_3$, hereafter we call this parameter compilation $\Lambda\text{CDM} - \ln A_s - n_s + \ln A_1 + \ln A_2 + \ln A_3$.

The marginalized mean scalar spectrum reconstructed from Planck + WP data is represented by the black solid curve in Fig. 1 and the corresponding $1 \sim 3\sigma$ error bars at the sampling points are denoted by the blue, red, and green segments, respectively. For comparison, we also show the

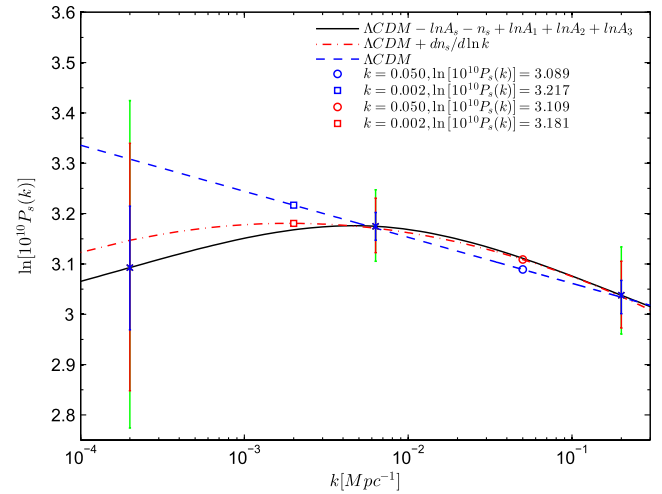


FIG. 1 (color online). Reconstruction of primordial scalar spectrum without BICEP2 data.

primordial scalar spectrum from the Planck marginalized mean vanilla ΛCDM and $\Lambda\text{CDM} + dn_s/d \ln k$ (scalar index running) with blue dashed and red dot-dashed curves. From Fig. 1, we can see that, first, our cubic spline interpolation result mimics the $\Lambda\text{CDM} + dn_s/d \ln k$ case; second, on the $k = 0.0002 \text{ Mpc}^{-1}$ scale, the simplest vanilla model is disfavored at the nearly 2σ level.

Adding the BICEP2 polarization data, we show the results in Fig. 2 for models including the tensor-to-scalar ratio r , i.e. $\Lambda\text{CDM} - \ln A_s - n_s + r + \ln A_1 + \ln A_2 + \ln A_3$. We find that, first of all, due to the anticorrelation between scalar and tensor amplitudes (see the bottom left subpanel of Fig. 8 in Appendix A), the large value of tensor-to-scalar ratio discovered by BICEP2 data will lead to the suppression of scalar amplitude on the large scales. This is also explicitly demonstrated in the top subpanel of Fig. 8 in Appendix A. As a result of deficit of scalar power

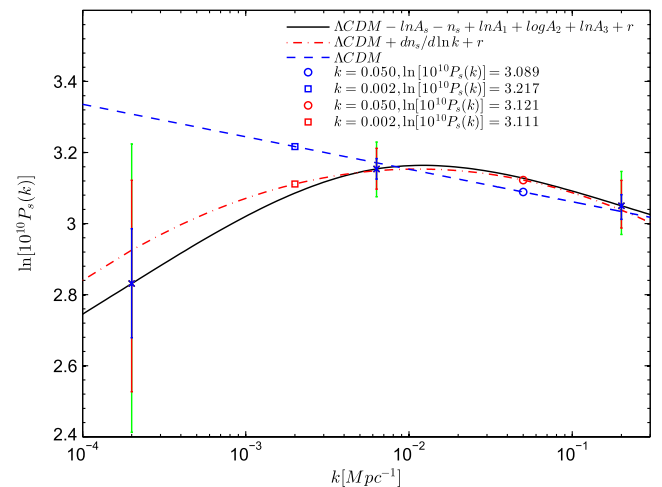


FIG. 2 (color online). Reconstruction of primordial scalar spectrum with BICEP2 data.

on the large scales, as shown in Fig. 2 the vanilla Λ CDM model (blue dashed curve) is strongly disfavored with $> 3\sigma$ confidence level on the $k = 0.0002 \text{ Mpc}^{-1}$ scale. A similar result is obtained by the authors of [51]. By using Planck and BICEP2 data, they found a distinct preference for a suppression of power in the scalar spectrum at large scales, $k \leq 10^{-3} \text{ Mpc}^{-1}$ via a linear spline reconstruction method. Second, by assuming the scale invariant tensor spectrum, our scalar spectrum cubic spline interpolation parametrization still gives a large tensor-to-scalar ratio $r = 0.21^{+0.10}_{-0.09}$ at 95% C.L., see Table II in Appendix A.

B. Tensor spectrum reconstruction

In the previous subsection, we have assumed the tensor spectrum is scale invariant. In this subsection we relax the assumption and use the same cubic spline interpolation method to reconstruct the shape of the tensor spectrum. Unlike the CMB temperature spectrum which is mainly sourced by the primordial scalar perturbations, the B-mode polarization anisotropy seeded by tensor perturbation is only detected by BICEP2 on the large scales with the polar spherical harmonic multipoles ranged $20 \leq \ell \leq 340$ (nine bandpowers). As the case for the scalar spectrum, here the tensor spectrum is also uniformly sampled with three points in the logarithmic scale of wave number, but only on the scales covered by BICEP2 observations. Consequently, we sample them at $k_1 = 0.002$, $k_2 = 0.0077$ and $k_3 = 0.03 \text{ Mpc}^{-1}$, respectively. The cosmological parameters we estimated are the six vanilla Λ CDM model parameters plus the extra three tensor amplitudes $\ln B_1$, $\ln B_2$ and $\ln B_3$.

In Fig. 3 we plot the primordial tensor spectra from the best-fit model of Λ CDM + $\ln B_1 + \ln B_2 + \ln B_3$ (black solid curve) and Λ CDM + $r + n_t$ (red dot-dashed curve) as well as the error bars at the sampling points of the cubic spline interpolation method. First of all, both the standard power-law and our cubic spline parametrizations favor a

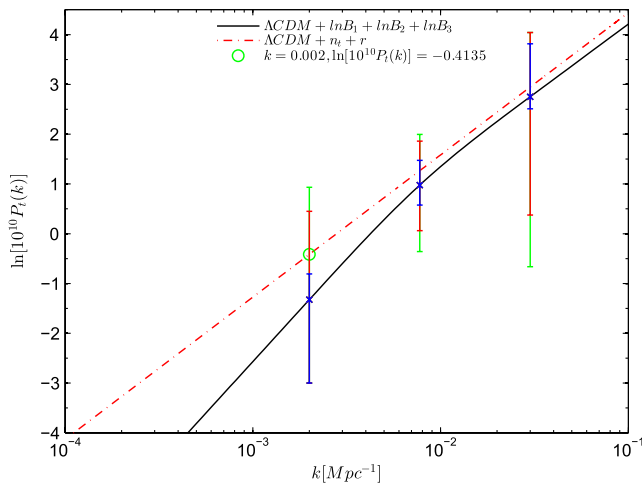


FIG. 3 (color online). Reconstruction of primordial tensor spectrum with BICEP2 data (nine bandpowers).

blue-tilt tensor spectrum. The former (see Table III in Appendix B) reports

$$r_{0.002} < 0.061, \quad 95\% \text{ C.L.} \quad (\text{nine bandpowers}), \quad (2)$$

$$n_t = 1.24^{+0.51}_{-0.58}, \quad 95\% \text{ C.L.} \quad (\text{nine bandpowers}), \quad (3)$$

which are qualitatively consistent with the results reported in [26–30]. For example, by using BICEP2 + Planck + WP + SN + BAO, the authors of [29] give $n_t = 0.822^{+0.240}_{-0.182}$ at 68% C.L. The small differences of marginalized mean value and confidence regime among those reported results come from the differences of data sets and the number of cosmological parameters adopted in those analyses. Our cubic spline interpolation method gives

$$r_{0.002} < 0.064, \quad 95\% \text{ C.L.} \quad (\text{nine bandpowers}). \quad (4)$$

Second, we notice that in our cubic spline interpolation method the slope of the tensor spectrum becomes larger in the low- k regime, but still is consistent with the power-law parametrization at the 2σ confidence level.

As we argued in the previous section, there exists an extraordinary power excess in the higher wave number regimes of BICEP2 data. Given this consideration, in what follows we only adopt the selected first five bandpower data of BICEP2 for our reconstruction. Based on the multipole ranges covered by these powerbands ($20 \leq \ell \leq 200$), we sample points at $k_1 = 0.002$, $k_2 = 0.0063$ and $k_3 = 0.02 \text{ Mpc}^{-1}$, respectively.

The reconstructed tensor spectra as well as error bars are shown in Fig. 4. First, from the power-law parametrization, we can see that the blue tensor spectra are still favored but with the tilt becomes smaller as expected:

$$r_{0.002} < 0.067, \quad 95\% \text{ C.L.} \quad (\text{five bandpowers}), \quad (5)$$

$$n_t = 1.20^{+0.56}_{-0.64}, \quad 95\% \text{ C.L.} \quad (\text{five bandpowers}). \quad (6)$$

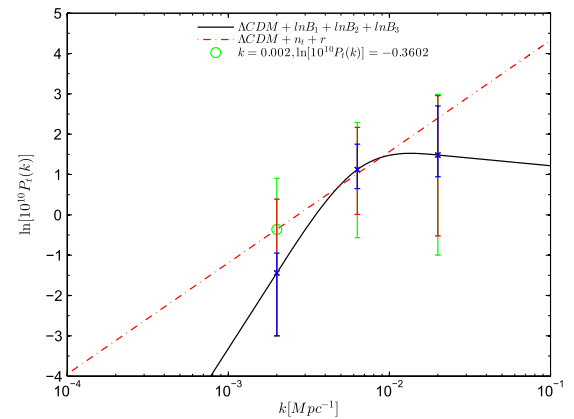


FIG. 4 (color online). Reconstruction of primordial tensor spectrum with BICEP2 data (five bandpowers).

Second, with only the first five bandpower data, unlike the simplest power-law parametrization, a nontrivial shape of tensor spectrum is obtained. Concretely, in the range of $k \in (0.002, 0.006)$ BICEP2 data favor a large tensor blue tilt, while when $k > 0.0063 \text{ Mpc}^{-1}$ the spectrum becomes almost flat. This is due to the fact that we do not use the last four bandpower data. The resulting tensor-to-scalar ratio in our cubic spline interpolation method is

$$r_{0.002} < 0.060, \quad 95\% \text{ C.L. (five bandpowers)}. \quad (7)$$

Because the above blue tensor tilt is significantly inconsistent with the standard inflationary prediction, we have to figure out its reason on the data analysis level. Notice that for now we always utilize Planck + WP + BICEP2 data compilation, so one natural guess is that this blue tensor tilt might reflect the tension among Planck, WMAP polarization and BICEP2 data sets. In order to justify our conjecture, we have to remove the above data sets one by one. Since we vary both the primordial spectrum and standard Λ CDM parameters, such as baryon ($\Omega_b h^2$), and cold dark matter density ($\Omega_c h^2$) etc., we have to keep the robust Planck temperature data in order to get well estimations of the Λ CDM parameters. Hence, we first remove the BICEP2, i.e. using Planck + WP, and further discard WMAP polarization data, i.e. only using Planck temperature data. However, due to the fact that CMB temperature data are insensitive to the reionization optical depth (τ), if we discard WMAP polarization data we have to include Gaussian prior on τ to break the well-known degeneracy between τ and the scalar amplitude A_s . Here we take the Gaussian prior as

$$\tau = 0.089 \pm 0.013. \quad (8)$$

Besides this, because the contribution of tensor spectra to CMB temperature anisotropies is only significant in the multipole range ($2 \leq \ell \leq 100$), when we use Planck + WP or Planck + τ prior data sets, we sample the k knots of tensor spectra in the range of (0.0002, 0.01).

The resulting primordial tensor spectrum shape, corresponding marginalized 1D/2D posterior distributions and parameter regimes are shown in Fig. 5, Fig. 10 and Table IV, respectively. First, we can see that the reconstructed tensor spectra from Planck + WP and Planck + τ prior are very similar, both for the central values and the marginalized error bars. So, we can draw the conclusion that WMAP low- ℓ polarization data are not crucial for the tensor reconstruction results. Second, as shown in Fig. 6 the error bars from Planck temperature data are quite large compared with those from the data compilation Planck + WP + BICEP2 (see the error bars at sampling knot $k = 0.01 \text{ Mpc}^{-1}$ in the dashed black curve and those at the second knot in the black solid curve in Fig. 6). It indicates that the current Planck temperature data are not robust to determine the shape of the primordial tensor

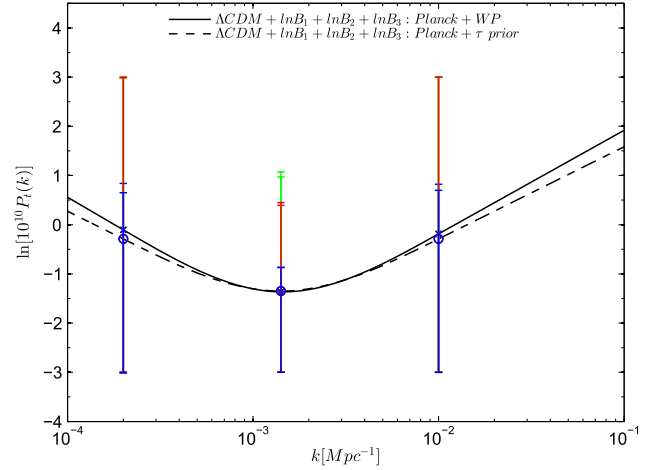


FIG. 5 (color online). Reconstruction of primordial tensor spectrum with Planck + WP and Planck + τ prior.

spectrum. The resulting tensor spectrum from only Planck temperature data could be any shape among red, blue or scale-invariant types. Third, when we compare the second knot in Planck + WP (dashed black curve) and the first left knot Planck + WP + BICEP2 results (solid black curve), Fig. 6 shows that both their central value and marginalized error bars are very close. It reflects the fact that the reconstructed tensor spectrum in the low- k regime is actually driven by Planck temperature data. Furthermore, considering the fact that the BICEP2 data dominate the high- k part, we conclude that our reconstructed blue tensor tilts are due to the tension between Planck and BICEP2 data sets, i.e. the fact that small tensor amplitude signals from Planck temperature data dominate the large scale reconstruction, while the large tensor amplitude signals from BICEP2 B-mode polarization data dominate the small scale reconstruction, leads to the resulting blue tensor tilt.

Finally, in order to give an intuitive impression of our reconstruction result, in Fig. 7 we plot the BB

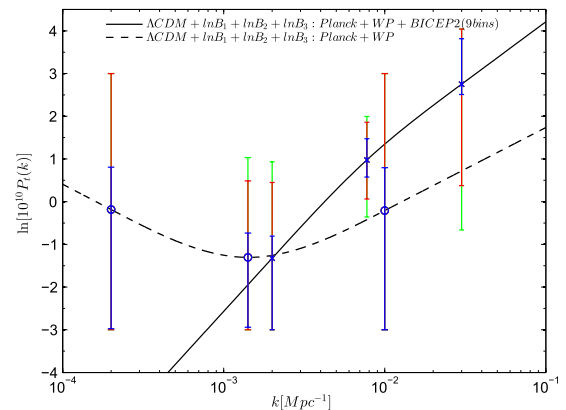


FIG. 6 (color online). Reconstruction of primordial tensor spectrum with/without BICEP2.

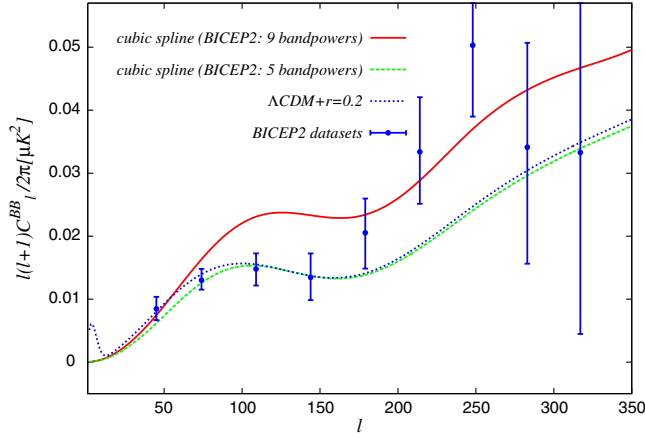


FIG. 7 (color online). CMB B-mode polarization autocorrelation spectrum C_{ℓ}^{BB} .

autocorrelation power spectrum of our marginalized mean models (listed in Table V of Appendix B) as well as the scale-invariant tensor spectrum with the $r = 0.2$ model against the BICEP2 bandpower data sets. We can see that in order to fit the BICEP2 data in the last four bandpowers, compared with the five bandpower reconstruction result (green dotted curve) and the scale-invariant one (blue dotted curves), the nine bandpower (red) curve grows up in the high- ℓ regime significantly. Furthermore, from Fig. 7 we can see that the marginalized mean BB power spectrum from five bandpowers (green dotted curve) is lower than the scale invariant one (blue dotted curve) in the multipole regime $\ell \in (250, 350)$. This is because, in the five bandpower case, the marginalized mean primordial tensor spectrum becomes nearly flat or even red tilt after the second knot (see Fig. 4).

IV. CONCLUSIONS

Starting with a purely phenomenological point of view, in this paper we have reconstructed the shape of the primordial scalar and tensor spectra by using the cubic spline interpolation method with Planck temperature and BICEP2 B-mode polarization data sets. We find that, due to the anticorrelation between scalar and tensor amplitudes on the large scales, the large value of tensor-to-scalar ratio discovered by BICEP2 data will lead to the suppression of scalar amplitude in this regime. Concretely, the vanishing scalar index running model is strongly disfavored by Planck + WP + BICEP2 data compilation with more than 3σ confidence level on the $k = 0.0002 \text{ Mpc}^{-1}$ scale. Furthermore, for the tensor spectrum reconstruction,

a blue-tilt spectrum is obtained no matter using only the first five bandpowers $n_t = 1.20^{+0.56}_{-0.64}$ (95% C.L.) or the full nine bandpowers $n_t = 1.24^{+0.51}_{-0.58}$ (95% C.L.) of BICEP2 data sets. Because of the large tensor tilt, compared with the large tensor-to-scalar ratio value ($r \sim 0.20$) under the scale-invariant assumption, our cubic spline interpolation method gives $r_{0.002} < 0.060$ (95% C.L.) and $r_{0.002} < 0.064$ (95% C.L.) by using the data sets Planck + WP + BICEP2 (five bandpowers) and (nine bandpowers), respectively. Finally, we also studied the data without BICEP2; we found that our resulting blue tensor tilt actually reflects the tension in the tensor amplitude between Planck (small amplitude but dominate the reconstruction on the large scale) and BICEP2 (large amplitude but dominate the reconstruction on the small scale) data sets.

Our results show that the conclusion of the blue-tilt tensor spectrum is very significant and independent of using power-law or cubic spline parametrizations. More important, this blue-tilt spectrum is not consistent with the prediction of the standard single field inflationary paradigm $n_t = -r/8$. On the one hand, it asks for a more careful cross-check with future experiments, such as the polarization data of Planck and Keck array. On the other hand, once this discovery is confirmed, it will lead to a paradigm revolution about our understanding of the early Universe.

ACKNOWLEDGMENTS

B. H. is indebted to Ana Achúcarro, Sabino Matarrese, Nicola Bartolo, Wessel Valkenburg and Frederico Arroja for various helpful discussions. He is supported by the Dutch Foundation for Fundamental Research on Matter (FOM). J. W. H., Z. K. G., and R. G. C. are partially supported by the project of Knowledge Innovation Program of Chinese Academy of Science, NSFC under Grants No. 11175225 and No. 11335012, and National Basic Research Program of China under Grants No. 2010CB832805 and No. 2010CB833004. R. G. C. is also supported by the Strategic Priority Research Program “The Emergence of Cosmological Structures” of the Chinese Academy of Sciences, Grant No. XDB09000000.

APPENDIX A: MARGINALIZED STATISTICS IN SCALAR SPECTRUM RECONSTRUCTION

Here we list the various marginalized statistical results for cubic spline interpolation and power-law parametrizations of scalar spectrum, including 1D, 2D marginalized posterior distribution, marginalized mean values as well as the 68% (or 95%) confidence levels.

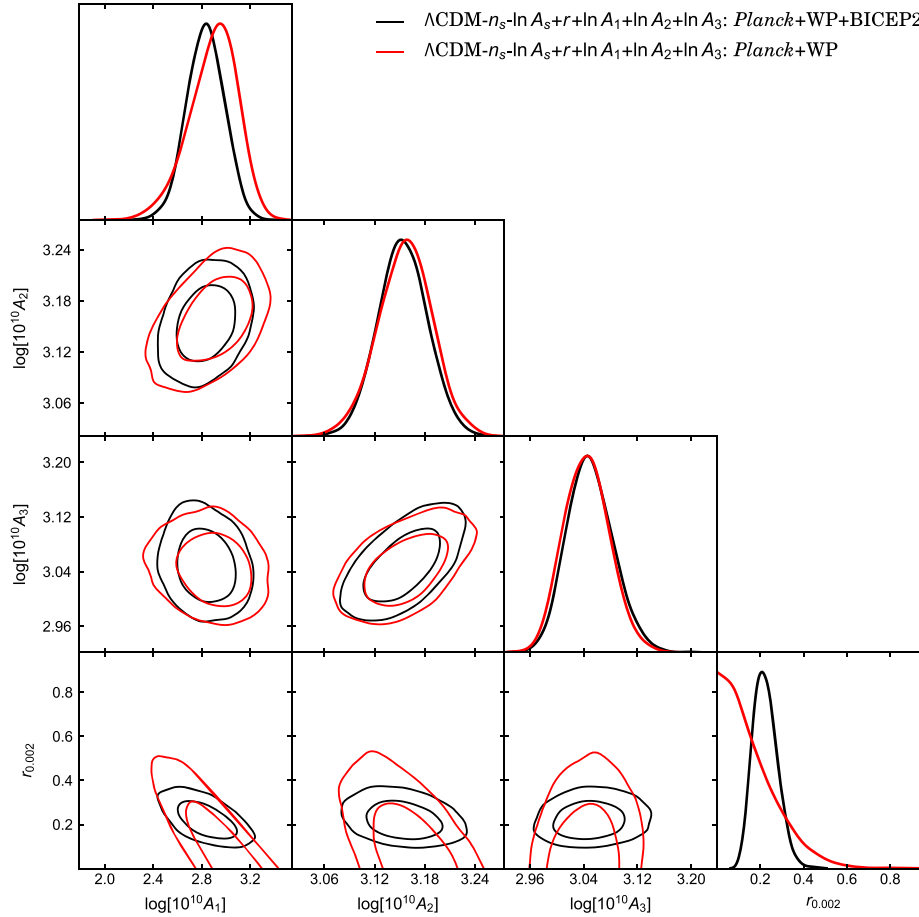


FIG. 8 (color online). 1D/2D posterior distribution of scalar spectrum reconstruction.

TABLE II. Mean values and 68% (or 95%) confidence limits for primary/derived parameters in the cubic spline and power-law parametrization of scalar spectrum.

| Parameters | $\Lambda\text{CDM} - n_s - \ln A_s + r + \ln A_1 + \ln A_2 + \ln A_3$ | | $\Lambda\text{CDM} + dn_s/d \ln k + r$ |
|-------------------------|---|---|---|
| | Planck + WP | Planck + WP + BICEP2 (nine bandpowers) | Planck + WP + BICEP2 (nine bandpowers) |
| | Mean \pm 68% C.L. | Mean \pm 68% C.L. | Mean \pm 68% C.L. |
| $100\Omega_b h^2$ | 2.224 ± 0.031 | 2.224 ± 0.030 | 2.238 ± 0.028 |
| $\Omega_c h^2$ | 0.1204 ± 0.0028 | 0.1202 ± 0.0027 | 0.1186 ± 0.0017 |
| $100\theta_{\text{MC}}$ | 1.04125 ± 0.00065 | 1.04133 ± 0.00063 | 1.04150 ± 0.00057 |
| τ | 0.103 ± 0.016 | 0.106 ± 0.017 | 0.105 ± 0.016 |
| $\ln(10^{10}A_s)$ | ... | ... | 3.122 ± 0.033 |
| n_s | ... | ... | 0.9600 ± 0.0063 |
| $dn_s/d \ln k$ | ... | ... | $-0.028^{+0.019}_{-0.021}$ (95% C.L.) |
| r | < 0.41 (95% C.L.) | $0.21^{+0.10}_{-0.09}$ (95% C.L.) | $0.20^{+0.08}_{-0.09}$ (95% C.L.) |
| $\ln(10^{10}A_1)$ | 2.89 ± 0.20 | 2.83 ± 0.15 | ... |
| $\ln(10^{10}A_2)$ | 3.157 ± 0.032 | 3.154 ± 0.029 | ... |
| $\ln(10^{10}A_3)$ | 3.045 ± 0.034 | 3.050 ± 0.034 | ... |
| Ω_m | 0.318 ± 0.018 | 0.316 ± 0.017 | 0.306 ± 0.010 |
| $H_0[\text{km/s/Mpc}]$ | 67.22 ± 1.27 | 67.34 ± 1.22 | 68.06 ± 0.79 |
| $\chi^2_{\text{min}}/2$ | 4901.833 | 4921.868 | 4924.052 |

APPENDIX B: MARGINALIZED STATISTICS IN TENSOR SPECTRUM RECONSTRUCTION

Here we list the various marginalized statistical results for cubic spline interpolation and power-law parametrizations of tensor spectrum, including 1D, 2D marginalized posterior distribution, marginalized mean values as well as the 68% (or 95%) confidence levels.

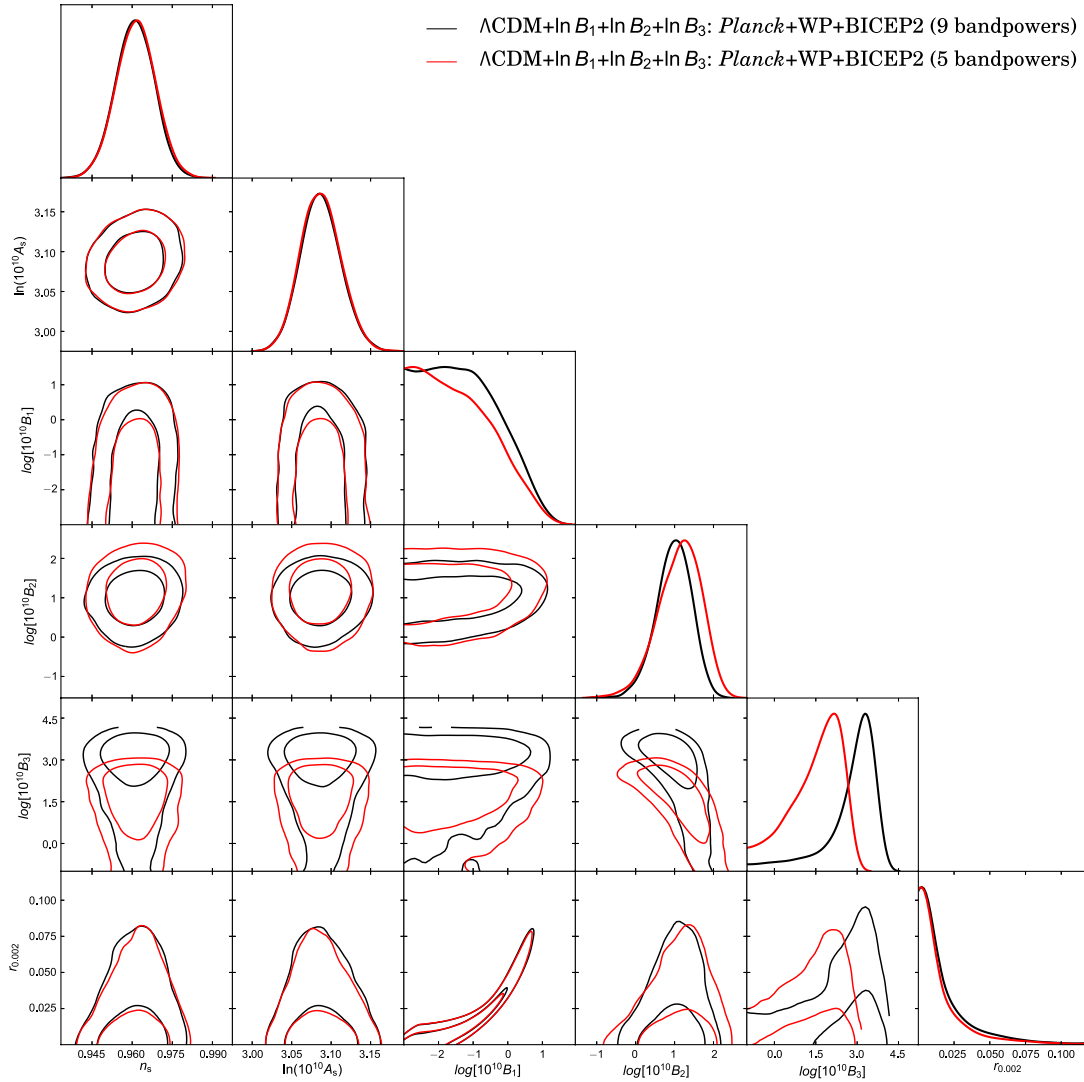


FIG. 9 (color online). 1D/2D posterior distribution of tensor spectrum reconstruction with BICEP2.

TABLE III. Mean values and 68% (or 95%) confidence limits for primary/derived parameters in the power-law parametrization of tensor spectrum.

| Parameters | Λ CDM + $r + n_t$ | |
|--------------------|--|--|
| | Planck + WP + BICEP2 (nine bandpowers) | Planck + WP + BICEP2 (five bandpowers) |
| | Mean \pm 68% C.L. | Mean \pm 68% C.L. |
| $100\Omega_b h^2$ | 2.200 ± 0.028 | 2.204 ± 0.028 |
| $\Omega_c h^2$ | 0.1194 ± 0.0026 | 0.1195 ± 0.0027 |
| $100\theta_{MC}$ | 1.04129 ± 0.00064 | 1.04127 ± 0.00063 |
| τ | 0.090 ± 0.013 | 0.089 ± 0.013 |
| n_s | 0.9611 ± 0.0073 | 0.9615 ± 0.0073 |
| $\ln(10^{10} A_s)$ | 3.087 ± 0.025 | 3.086 ± 0.025 |
| $r_{0.05}$ | < 2.00 (95% C.L.) | < 2.00 (95% C.L.) |
| n_t | $1.24^{+0.51}_{-0.58}$ (95% C.L.) | $1.20^{+0.56}_{-0.64}$ (95% C.L.) |
| Ω_m | 0.313 ± 0.016 | 0.313 ± 0.016 |
| H_0 [km/s/Mpc] | 67.38 ± 1.19 | 67.40 ± 1.11 |
| $r_{0.002}$ | < 0.061 (95% C.L.) | < 0.067 (95% C.L.) |
| $\chi^2_{\min}/2$ | 4920.773 | 4909.861 |

TABLE IV. Mean values and 68% (or 95%) confidence limits for primary/derived parameters in the tensor spectrum cubic spline reconstruction.

| Parameters | Λ CDM + $\ln B_1 + \ln B_2 + \ln B_3$ | |
|--------------------|---|--|
| | Planck + WP + BICEP2 (nine bandpowers) | Planck + WP + BICEP2 (five bandpowers) |
| | Mean \pm 68% C.L. | Mean \pm 68% C.L. |
| $100\Omega_b h^2$ | 2.202 ± 0.028 | 2.202 ± 0.028 |
| $\Omega_c h^2$ | 0.1194 ± 0.0026 | 0.1195 ± 0.0026 |
| $100\theta_{MC}$ | 1.04130 ± 0.00063 | 1.04125 ± 0.00062 |
| τ | 0.090 ± 0.013 | 0.090 ± 0.013 |
| n_s | 0.9610 ± 0.0071 | 0.9614 ± 0.0072 |
| $\ln(10^{10} A_s)$ | 3.087 ± 0.025 | 3.087 ± 0.025 |
| $\ln(10^{10} B_1)$ | < 0.45 (95% C.L.) | < 0.39 (95% C.L.) |
| $\ln(10^{10} B_2)$ | $0.98^{+0.88}_{-0.92}$ (95% C.L.) | $1.12^{+1.05}_{-1.02}$ (95% C.L.) |
| $\ln(10^{10} B_3)$ | $2.75^{+1.29}_{-2.37}$ (95% C.L.) | $1.48^{+1.48}_{-2.00}$ (95% C.L.) |
| Ω_m | 0.313 ± 0.016 | 0.314 ± 0.016 |
| H_0 [km/s/Mpc] | 67.43 ± 1.17 | 67.37 ± 1.17 |
| $r_{0.002}$ | < 0.064 (95% C.L.) | < 0.060 (95% C.L.) |
| $\chi^2_{\min}/2$ | 4920.558 | 4909.799 |

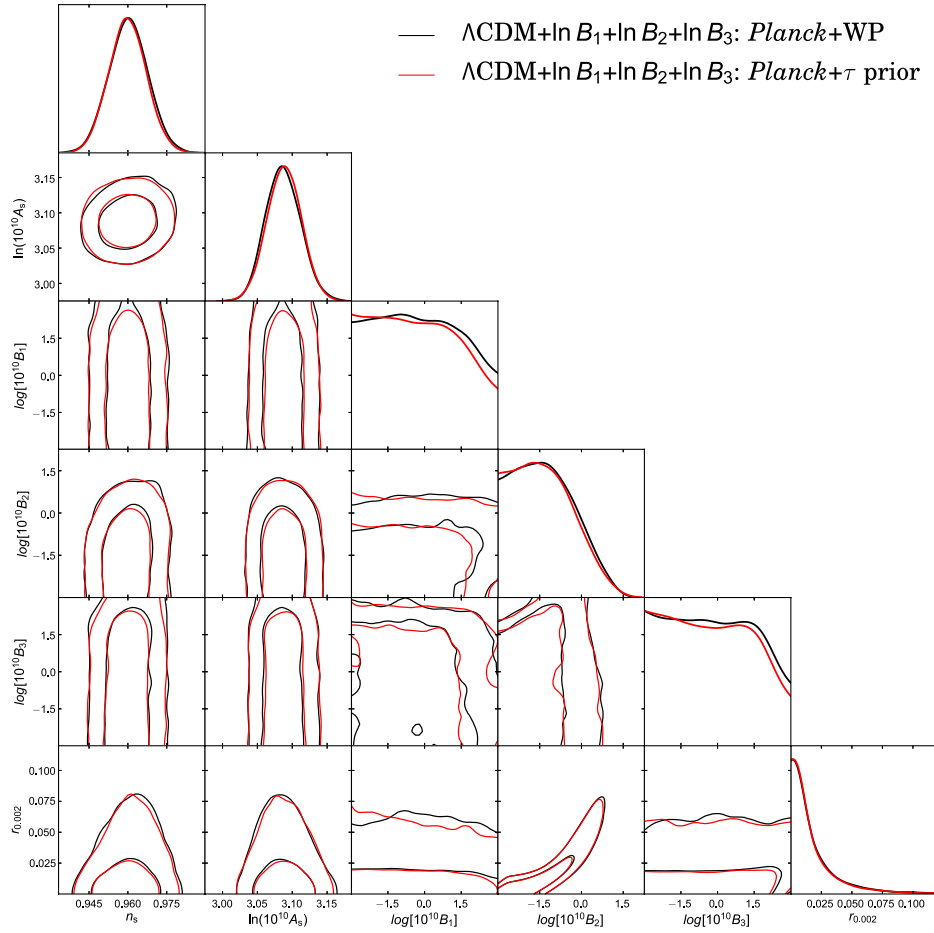


FIG. 10 (color online). 1D/2D posterior distribution of tensor spectrum reconstruction without BICEP2.

TABLE V. Mean values and 68% (or 95%) confidence limits for primary/derived parameters in the tensor spectrum cubic spline reconstruction.

| Parameters | $\Lambda\text{CDM} + \ln B_1 + \ln B_2 + \ln B_3$ | |
|-------------------------|---|----------------------------|
| | Planck + WP | Planck + τ prior |
| | Mean \pm 68% C.L. | Mean \pm 68% C.L. |
| $100\Omega_b h^2$ | 2.204 ± 0.028 | 2.203 ± 0.028 |
| $\Omega_c h^2$ | 0.1200 ± 0.0028 | 0.1201 ± 0.0027 |
| $100\theta_{\text{MC}}$ | 1.04122 ± 0.00063 | 1.04119 ± 0.00063 |
| τ | 0.089 ± 0.013 | 0.090 ± 0.012 |
| n_s | 0.9603 ± 0.0074 | 0.9599 ± 0.0071 |
| $\ln(10^{10} A_s)$ | 3.087 ± 0.025 | 3.089 ± 0.024 |
| $\ln(10^{10} B_1)$ | $(-3.00, 3.00)$ (95% C.L.) | $(-3.00, 3.00)$ (95% C.L.) |
| $\ln(10^{10} B_2)$ | $(-3.00, 0.49)$ (95% C.L.) | $(-3.00, 0.45)$ (95% C.L.) |
| $\ln(10^{10} B_3)$ | $(-3.00, 3.00)$ (95% C.L.) | $(-3.00, 3.00)$ (95% C.L.) |
| Ω_m | 0.317 ± 0.017 | 0.317 ± 0.016 |
| $H_0[\text{km/s/Mpc}]$ | 67.20 ± 1.22 | 67.14 ± 1.17 |
| $r_{0.002}$ | < 0.064 (95% C.L.) | < 0.062 (95% C.L.) |
| $\chi^2_{\text{min}}/2$ | 4902.387 | 3895.305 |

- [1] P. A. R. Ade *et al.* (BICEP2 Collaboration), *Phys. Rev. Lett.* **112**, 241101 (2014).
- [2] P. A. R. Ade *et al.* (Planck Collaboration), [arXiv:1303.5082](https://arxiv.org/abs/1303.5082).
- [3] W. Hu and M. J. White, *Phys. Rev. D* **56**, 596 (1997).
- [4] K. M. Smith, C. Dvorkin, L. Boyle, N. Turok, M. Halpern, G. Hinshaw, and B. Gold, [arXiv:1404.0373](https://arxiv.org/abs/1404.0373).
- [5] G. Hinshaw *et al.* (WMAP Collaboration), *Astrophys. J. Suppl. Ser.* **208**, 19 (2013).
- [6] S. Das, T. Louis, M. R. Nolta, G. E. Addison, E. S. Battistelli, J. R. Bond, E. Calabrese, D. C. M. J. Devlin *et al.*, *J. Cosmol. Astropart. Phys.* **04** (2014) 014.
- [7] R. Keisler, C. L. Reichardt, K. A. Aird, B. A. Benson, L. E. Bleem, J. E. Carlstrom, C. L. Chang, H. M. Cho *et al.*, *Astrophys. J.* **743**, 28 (2011).
- [8] K. T. Story, C. L. Reichardt, Z. Hou, R. Keisler, K. A. Aird, B. A. Benson, L. E. Bleem, J. E. Carlstrom *et al.*, *Astrophys. J.* **779**, 86 (2013).
- [9] C. L. Reichardt, L. Shaw, O. Zahn, K. A. Aird, B. A. Benson, L. E. Bleem, J. E. Carlstrom, C. L. Chang *et al.*, *Astrophys. J.* **755**, 70 (2012).
- [10] V. c. Miranda, W. Hu, and P. Adshead, *Phys. Rev. D* **89**, 101302(R) (2014).
- [11] D. K. Hazra, A. Shafieloo, G. F. Smoot, and A. A. Starobinsky, *J. Cosmol. Astropart. Phys.* **06** (2014) 061.
- [12] R. Bousso, D. Harlow, and L. Senatore, [arXiv:1404.2278](https://arxiv.org/abs/1404.2278).
- [13] D. K. Hazra, A. Shafieloo, and G. F. Smoot, [arXiv:1404.0360](https://arxiv.org/abs/1404.0360).
- [14] M. Kawasaki and S. Yokoyama, *J. Cosmol. Astropart. Phys.* **05** (2014) 046.
- [15] M. Kawasaki, T. Sekiguchi, T. Takahashi, and S. Yokoyama, [arXiv:1404.2175](https://arxiv.org/abs/1404.2175).
- [16] E. Giusarma, E. Di Valentino, M. Lattanzi, A. Melchiorri, and O. Mena, [arXiv:1403.4852](https://arxiv.org/abs/1403.4852).
- [17] J.-F. Zhang, Y.-H. Li, and X. Zhang, [arXiv:1403.7028](https://arxiv.org/abs/1403.7028).
- [18] C. Dvorkin, M. Wyman, D. H. Rudd, and W. Hu, [arXiv:1403.8049](https://arxiv.org/abs/1403.8049).
- [19] C. R. Contaldi, M. Peloso, and L. Sorbo, *J. Cosmol. Astropart. Phys.* **07** (2014) 014.
- [20] B. Freivogel, M. Kleban, M. R. Martinez, and L. Susskind, [arXiv:1404.2274](https://arxiv.org/abs/1404.2274).
- [21] H. Firouzjahi and M. H. Namjoo, [arXiv:1404.2589](https://arxiv.org/abs/1404.2589).
- [22] Y.-F. Cai, J.-O. Gong, and S. Pi, [arXiv:1404.2560](https://arxiv.org/abs/1404.2560).
- [23] C. Cheng, Q.-G. Huang, and W. Zhao, *Sci. China Phys. Mech. Astron.* **57**, 1460 (2014).
- [24] S. Choudhury and A. Mazumdar, [arXiv:1403.5549](https://arxiv.org/abs/1403.5549).
- [25] S. Hotchkiss, A. Mazumdar, and S. Nadathur, *J. Cosmol. Astropart. Phys.* **02** (2012) 008.
- [26] M. Gerbino, A. Marchini, L. Pagano, L. Salvati, E. Di Valentino, and A. Melchiorri, [arXiv:1403.5732](https://arxiv.org/abs/1403.5732).
- [27] F. Wu, Y. Li, Y. Lu, and X. Chen, *Sci. China Phys. Mech. Astron.* **57**, 1449 (2014).
- [28] C. Cheng and Q.-G. Huang, [arXiv:1403.7173](https://arxiv.org/abs/1403.7173).
- [29] H. Li, J.-Q. Xia, and X. Zhang, [arXiv:1404.0238](https://arxiv.org/abs/1404.0238).
- [30] B. Chang and L. Xu, [arXiv:1404.1558](https://arxiv.org/abs/1404.1558).
- [31] M. Baldi, F. Finelli, and S. Matarrese, *Phys. Rev. D* **72**, 083504 (2005).
- [32] Y.-S. Piao and Y.-Z. Zhang, *Phys. Rev. D* **70**, 063513 (2004).
- [33] T. Kobayashi, M. Yamaguchi, and J. 'i. Yokoyama, *Phys. Rev. Lett.* **105**, 231302 (2010).
- [34] R. H. Brandenberger, A. Nayeri, and S. P. Patil, [arXiv:1403.4927](https://arxiv.org/abs/1403.4927).
- [35] P. Creminelli, M. A. Luty, A. Nicolis, and L. Senatore, *J. High Energy Phys.* **12** (2006) 080.
- [36] P. Creminelli and L. Senatore, *J. Cosmol. Astropart. Phys.* **11** (2007) 010.
- [37] E. I. Buchbinder, J. Khoury, and B. A. Ovrut, *Phys. Rev. D* **76**, 123503 (2007).
- [38] J.-Q. Xia, Y.-F. Cai, H. Li, and X. Zhang, *Phys. Rev. Lett.* **112**, 251301 (2014).
- [39] T. Qiu, [arXiv:1404.3060](https://arxiv.org/abs/1404.3060).
- [40] Y.-S. Piao, B. Feng, and X.-m. Zhang, *Phys. Rev. D* **69**, 103520 (2004).
- [41] Z.-G. Liu, Z.-K. Guo, and Y.-S. Piao, *Phys. Rev. D* **88**, 063539 (2013).
- [42] J.-O. Gong, [arXiv:1403.5163](https://arxiv.org/abs/1403.5163).
- [43] Y. Wang and W. Xue, [arXiv:1403.5817](https://arxiv.org/abs/1403.5817).
- [44] C. Sealton, L. Verde, and R. Jimenez, *Phys. Rev. D* **72**, 103520 (2005).
- [45] L. Verde and H. V. Peiris, *J. Cosmol. Astropart. Phys.* **07** (2008) 009.
- [46] H. V. Peiris and L. Verde, *Phys. Rev. D* **81**, 021302 (2010).
- [47] Z.-K. Guo, D. J. Schwarz, and Y.-Z. Zhang, *J. Cosmol. Astropart. Phys.* **08** (2011) 031.
- [48] Z.-K. Guo and Y.-Z. Zhang, *J. Cosmol. Astropart. Phys.* **11** (2011) 032.
- [49] Z.-K. Guo and Y.-Z. Zhang, *Phys. Rev. D* **85**, 103519 (2012).
- [50] G. Aslanyan, L. C. Price, K. N. Abazajian, and R. Easther, [arXiv:1403.5849](https://arxiv.org/abs/1403.5849).
- [51] K. N. Abazajian, G. Aslanyan, R. Easther, and L. C. Price, [arXiv:1403.5922](https://arxiv.org/abs/1403.5922).
- [52] J. A. Vazquez, M. Bridges, M. P. Hobson, and A. N. Lasenby, *J. Cosmol. Astropart. Phys.* **06** (2012) 006.
- [53] J. A. Vazquez, M. Bridges, Y.-Z. Ma, and M. P. Hobson, *J. Cosmol. Astropart. Phys.* **08** (2013) 001.
- [54] P. A. R. Ade *et al.* (Planck Collaboration), [arXiv:1303.5075](https://arxiv.org/abs/1303.5075).
- [55] P. A. R. Ade *et al.* (Planck Collaboration), [arXiv:1303.5076](https://arxiv.org/abs/1303.5076).
- [56] A. Lewis, A. Challinor, and A. Lasenby, *Astrophys. J.* **538**, 473 (2000).
- [57] A. Lewis and S. Bridle, *Phys. Rev. D* **66**, 103511 (2002).